Master's Thesis

Title

Proposal and Evaluation of Wireless Signal Mapping and Navigation for Mobile Robotic Cellular Base Stations

Supervisor

Associate Professor Shin'ichi Arakawa

Author

Atsuhisa Hazama

February 3rd, 2025

Department of Information Networking

Graduate School of Information Science and Technology

Osaka University

Master's Thesis

Proposal and Evaluation of Wireless Signal Mapping and Navigation for Mobile Robotic Cellular Base Stations

Atsuhisa Hazama

Abstract

With the advancement of communication technology in recent years, the demand for multimedia services has been increasing in various fields such as transportation, entertainment, and healthcare. Consequently, mobile communication systems are being utilized in a wide range of domains. Under current regulations, base stations are generally required to be fixed installations. However, if mobile base stations can be deployed, various applications can be expected. For example, mobile base stations can be deployed in non-residential areas where commercial cellular networks are not available, such as some mountainous regions and remote islands, as well as in situations where communication is essential, such as construction work in tunnels or high-rise buildings.

However, in densely populated environments such as events, communication quality may deteriorate due to the movement of crowds or the emergence of temporary obstacles, making it difficult to maintain stable connectivity. Furthermore, indoor environments exhibit significant radio wave attenuation and multipath interference, which are particularly challenging issues in 5G networks. Currently, when adjusting the position of a mobile base station dynamically, multiple communication terminals may connect simultaneously, leading to a situation where certain terminals are more likely to experience a decline in communication quality. Additionally, real-time measurement of signal quality by mobile base stations is costly, and directly observing the entire area is impractical. To address these challenges, a control technology for mobile base stations is required that can estimate the communication quality of terminals with high accuracy based on limited observation data, enabling real-time measurement of dynamic communication quality changes and ensuring fair communication quality among multiple terminals.

In this thesis, we propose and develop a mobility control method for mobile base stations to achieve fair communication quality among multiple terminals. By employing Bayesian Compressive Sensing (BCS), we construct a Superimposed Signal Map (SSM) using limited observation data, enabling the dynamic determination of optimal mobile base station placement to enhance communication quality. The evaluation results confirm that the proposed method significantly enhances communication quality. The average RSRP increased by 110.7 dBm for two terminals and 80.9 dBm for three terminals, with the weakest terminals also seeing substantial improvements. Uncertainty reduction converged after 7 iterations for two terminals and 12 iterations for three terminals, and the number of grids that inspects is decreased to 24.7% and 42.4% respectively. The visual analysis shows that the Estimated RSRP closely matches the ground-truth distribution, and the mobile base station moved to locations within seven grids for two terminals and four grids for three terminals of the ground-truth maximum RSRP points, demonstrating effective mobility control. This method offers a practical approach to optimizing mobile base station placement in 5G environments, with applications in disaster response, large-scale events, and temporary network deployments.

Keywords

5th Generation Mobile Communication System
Mobile Robotic Cellular Base Stations
Bayesian Compressive Sensing
Superimposed Signal Map
Radio Environment Sensing
Integrated Access and Backhaul

Contents

List of Figures

List of Tables

1 Introduction

With the advancement of communication technology in recent years, the demand for multimedia services has been increasing in various fields such as transportation, entertainment, and healthcare. Consequently, mobile communication systems are being utilized in a wide range of domains. In particular, when communication terminals are not stationary but mobile, the use of mobile communication systems based on 5G technology becomes indispensable.

For instance, in efforts to enhance agricultural operations, automated tractors and drones connected to cellular networks are being considered to navigate farms and perform agricultural tasks in place of human workers [1]. Additionally, in the postal and logistics sectors, autonomous delivery robots connected to cellular networks are being developed to travel public roads and deliver packages to designated locations [2]. In these cases, base stations are fixed installations, and communication terminals operate within the coverage area of the base stations.

Under current regulations, base stations are generally required to be fixed installations. However, if mobile base stations can be deployed, various applications can be expected. For example, mobile base stations can be deployed in non-residential areas where commercial cellular networks are not available, such as some mountainous regions and remote islands, as well as in situations where communication is essential, such as construction work in tunnels or high-rise buildings. Additionally, in disaster scenarios where the environmental conditions assumed for fixed base stations change, rendering them inoperable, the deployment of mobile base stations can be highly effective.

Research on vehicle-mounted base stations, where base stations are installed on large vehicles such as trucks, has explored their use in disaster recovery when fixed base stations become inoperable due to earthquakes and other disasters. These mobile base stations can be dispatched to disaster-stricken areas to temporarily restore communication services. Furthermore, they have been considered for supplementing communication infrastructure at large-scale events such as fireworks festivals and outdoor music concerts [3].

However, in densely populated environments such as events, communication quality may deteriorate due to the movement of crowds or the emergence of temporary obstacles,

making it difficult to maintain stable connectivity.

Moreover, 5G networks face several distinct challenges in indoor environments. First, the attenuation of radio waves is significant. The high-frequency bands used in 5G communication, particularly the millimeter-wave bands, are easily obstructed by building materials such as walls, floors, and ceilings [4]. As a result, dead zones where radio signals cannot reach occur, significantly degrading communication quality. Second, due to the strong directivity of millimeter waves, obstacles and terminal movements have a substantial impact on communication quality. For example, the movement of furniture or people can block signals, leading to communication disruptions. Third, there is the issue of multipath interference [5]. In indoor environments, radio waves reflect off walls and ceilings, reaching terminals through multiple paths, which causes signal interference and degrades communication quality. This results in "dead spots," where communication quality is extremely poor in specific locations. Fourth, there is the problem of radio wave density and bandwidth limitations. When a large number of terminals concentrate in one location, bandwidth usage can become excessive, leading to significant reductions in communication speed. To overcome these challenges, it is necessary to develop a technology that can capture the communication quality of multiple terminals in real time and control the movement of mobile base stations based on the communication quality conditions of each terminal.

Currently, when adjusting the position of a mobile base station dynamically, multiple communication terminals may connect simultaneously, leading to a situation where certain terminals are more likely to experience a decline in communication quality. This issue is influenced by various factors, such as the distance between the base station and terminals, the placement of obstacles, and signal interference among terminals. For example, when a mobile base station moves too close to certain terminals, the distance to other terminals increases, which can result in lower communication speeds and unstable connections. Such an imbalance in communication quality not only degrades overall service quality but also creates unfair disadvantages for some users, making it a significant issue from an equity perspective.

Additionally, real-time measurement of signal quality by mobile base stations is costly, and directly observing the entire area is impractical. To address these challenges, a control

technology for mobile base stations is required that can estimate the communication quality of terminals with high accuracy based on limited observation data, enabling real-time measurement of dynamic communication quality changes and ensuring fair communication quality among multiple terminals.

In this thesis, we propose a dynamic mobility control method for mobile base stations utilizing 5G communication technology to improve communication quality and ensure fairness. Our objective is to adapt to dynamic environmental changes in both indoor and outdoor environments while overcoming the challenges of signal attenuation and strong directivity inherent in 5G networks, thereby mitigating communication disruptions and quality degradation.

Specifically, we develop a method that efficiently constructs a Superimposed Signal Map from limited observation data using Bayesian Compressive Sensing (BCS) [6] and dynamically controls the placement of mobile base stations to ensure fair communication quality among multiple terminals. Furthermore, we evaluate the effectiveness of the proposed method through simulations and verify its applicability in various scenarios such as disaster recovery and large-scale events.

The remainder of this thesis is structured as follows. Section 2 presents the experimental setup and preliminary validation of the proposed mobility control method using a small-scale 5G mobile base station. Section 3 introduces the proposed wireless signal mapping and mobility control methods, detailing the construction of the Superimposed Signal Map (SSM) and the movement control method using Bayesian Compressive Sensing (BCS). Section 4 describes the evaluation methodology and presents the simulation results demonstrating the effectiveness of the proposed approach. Finally, Section 5 concludes the thesis by summarizing the findings and discussing potential future research directions.

2 Demonstration of Mobility Control for Mobile Robotic Cellular Base Stations Using Radio Environment Sensing

This section describes the experiments conducted on the small-scale 5G mobile base station and its mobility control, which were developed as part of a special research project.

2.1 Construction of Mobile Robotic Cellular Base Stations

This subsection explains the components of the small-scale 5G mobile base station, signal quality measurement, and mobility control methods. Additionally, it discusses IAB (3GPP R17), which is utilized as the backhaul technology for the mobile base station.

2.1.1 Components of the Mobile Base Station

In this thesis, a mobile base station was constructed and verified by mounting a base station on the Double3 mobile robot from Double Robotics [7]. Double3 is an autonomous vehicle equipped with an NVIDIA Jetson, capable of performing real-time image classification, object detection, and self-localization applications.

The components of the constructed mobile base station are summarized in Table 1. The logical configuration of the mobile base station using the equipment listed in Table 1 is shown in Figure 1.

Table 1: Components of the Mobile Base Station

Component		Details
Mobile Platform		Double3
5GC		Raspberry Pi 4
Base Station	gNB	Compact PC with AMD Ryzen 7
	RU	USRP B210 mini
	Antenna	Visible light-transparent antenna
Power Supply		Mobile Battery

Table 2: Specifications of the Compact PC with AMD Ryzen 7

CPU	Quad-core AMD Ryzen 7 3750H
CPU Clock Speed	2.3GHz
Chassis Dimensions	Width 12.4 cm, Height 11.2 cm, Depth 4 cm
Power Consumption	Approx. 65W

2.1.2 Base Station

This subsection describes the physical structure and specifications of the base station. In this thesis, a mobile base station was constructed and verified by mounting a base station on the Double3 autonomous vehicle. The base station consists of four components: gNB, 5GC, RU, and an antenna.

For the gNB, a compact PC was used, while a Raspberry Pi 4 was employed for the 5GC. The RU was implemented using a USRP B210. The antenna used was a 3.7/4.7 GHz band MIMO-compatible V-polarized visible light-transparent antenna, which is omnidirectional in the horizontal plane. Additionally, the gNB was implemented using a modified version of the open-source software OAI [8], while the 5G-Core was implemented using a customized version of Open5GS [9]. The specifications of the compact PC and Raspberry Pi 4 are summarized in Tables 2 and 3, respectively.

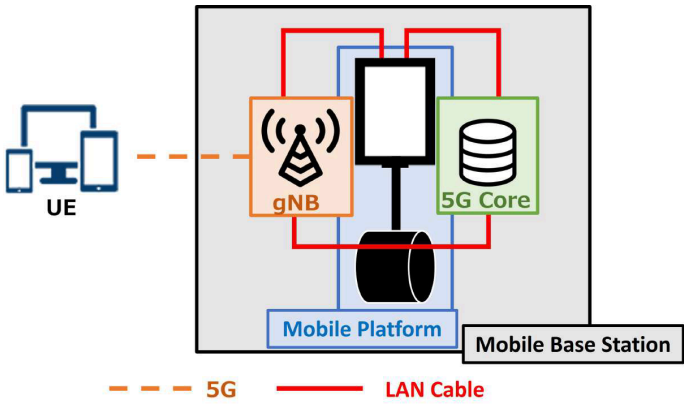

Figure 1: Configuration of the Mobile Base Station

Table 3: Specification of Raspberry Pi 4

CPU	Quad-core Cortex-A72 (ARM v8)
CPU Clock Speed	1.5GHz
Power Consumption	Approx. 15W

2.1.3 Mobile Platform

This subsection describes the control method of the Double3 platform. By switching to developer mode, it is possible to access developer-specific features on Double3.

Double3 is equipped with an Nvidia Jetson TX2 4GB system-on-module, which is connected to various built-in sensors and devices, allowing the execution of custom-developed code. Additionally, since Double3 runs Ubuntu 18.04 on an aarch64 architecture, code can be written in any language compatible with this platform.

The core software of Double3 runs as a system service called "d3." The d3 service includes a control API that enables movement by a specified amount, acquisition of position coordinates, and camera operation. By writing and executing code, commands can be sent and events received, allowing the use of the d3 control API. Furthermore, all commands and events are transmitted via standard Unix domain sockets.

Figure 2: Mobile Base Station

2.1.4 Power Supply

In this thesis, the mobile base station needs to operate autonomously. Since Double3 is rechargeable, charging before experiments is sufficient. However, the base station requires a dedicated power supply. Therefore, a mobile battery is used as the power source for the base station, with a capacity of 87.04Wh. The mobile battery is connected via a 100V AC output terminal to supply power to the compact PC used as the gNB and via a USB-C output terminal to power the Raspberry Pi 4, which serves as the 5GC.

2.1.5 Specifications of the Mobile Base Station

The mobile base station used in this thesis consists of the Double3 platform carrying the base station and power supply. The base station operates by drawing power from the mobile battery. A photograph of the mobile base station is shown in Figure 2.

The center frequency of the radio signal used by the mobile base station was set to 3.433GHz. The bandwidth was set to 20MHz (RB51), and the maximum MCS value was set to 0. Under these conditions, the system operated for approximately 80 minutes.

2.1.6 Signal Quality Measurement

The Measurement Report function, used for handovers between base stations, is utilized to measure the signal quality received by terminals. The Measurement Report is an RRC-layer feature in 5G communication. Thus, by extracting information from the RRC layer, the application layer of the base station in the mobile base station manages the received signal strength of each terminal.

In the base station mounted on the mobile platform, the Measurement Report collects RSRP (Reference Signal Received Power), RSRQ, and SINR for each terminal at fixed intervals. The collection interval can be set between 120ms and 30 minutes, but in this thesis, it was set to 240ms.

Although channel state information (CSI) or data from OFDM signal processing could be used to acquire signal quality at shorter intervals, this would increase processing complexity, power consumption, and system weight. Therefore, the Measurement Report function was chosen for obtaining received signal strength. The compact PC used as the gNB logs and continuously updates RNTI (Radio Network Temporary Identifier) for the connected User Equipment (UE), along with the collected RSRP, RSRQ, and SINR, in real-time.

2.1.7 Mobility Control API

This subsection describes the commands from Double3's control API [10] necessary for mobility control, as well as the mobility control API program developed for this purpose.

Since the Measurement Report function operates at the RRC layer in 5G communication, the information obtained from the RRC layer must be passed to the mobility control API. The mobility control API then calculates the required movement amount and executes the mobility control.

The `DRNavigateModule.arrive` command is responsible for monitoring events that indicate the completion of movements issued by the navigation system. By detecting when a movement is completed, this command ensures that the mobile base station can transition smoothly between different movement phases. The `DRPose.pose` command provides the absolute position of Double3 within the coordinate system, enabling real-time tracking of

its location. This function relies on self-localization using wheel rotation and an Inertial Measurement Unit (IMU). Finally, the `navigate.target` command treats the movement plane of the mobile platform as a two-dimensional coordinate system and issues movement commands based on target coordinates, which include both forward and lateral displacement, as well as the final orientation after movement. It allows specifying movement using either relative coordinates from the current position or absolute coordinates. In this thesis, all movement commands were issued using absolute coordinates. However, in practice, a discrepancy of approximately 50 cm between the specified and actual movement distances was observed. To correct this error, an error compensation mechanism was applied to refine movement accuracy.

2.1.8 Mobility Control Using the Mobility Control API

To enable mobility control of the mobile base station based on the received signal quality of multiple terminals, the mobility control API was implemented in Python. Double3 and the base station are connected via a wired LAN cable, and by establishing an SSH connection from Double3 to the compact PC serving as the base station, terminal information can be retrieved. The mobility control API is executed on Double3 to perform movement adjustments.

The mobility control process consists of two main steps. First, the mobile base station moves at fixed distance intervals while measuring the received signal strength of multiple terminals, constructing a Superimposed Signal Map that represents the received signal strength at each location. Then, based on the constructed Superimposed Signal Map, the system determines the optimal location that maximizes the average received signal strength among multiple terminals, and the mobile base station moves to that position accordingly.

The signal quality data obtained through measurement is managed at the application layer of the base station, and Double3 retrieves this data via an SSH connection. In this thesis, mobility control and Superimposed Signal Map construction were conducted using one-dimensional (linear) movement of the mobile base station. This approach was chosen because performing radio environment sensing and mobility control in a two-dimensional or three-dimensional space makes it difficult to comprehensively measure signal quality

across a wide area solely through the movement of the mobile base station.

2.2 Mobility Control Based on Radio Environment Sensing Using Mobile Robotic Cellular Base Stations

This subsection presents the experiments and results of mobility control based on radio environment sensing using the constructed mobile base station. It also discusses the necessity of two-dimensional and three-dimensional Superimposed Signal Map construction, which is crucial for mobile base station operations.

The Superimposed Signal Map is first constructed, followed by mobility control based on the estimated signal distribution. To validate the proposed method, a mobile communication system was implemented, and its performance was evaluated through experiments.

2.2.1 Superimposed Signal Map Construction via Radio Environment Sensing

In the experimental environment described in Section 2.2.3, the Superimposed Signal Map is constructed by measuring the signal quality between terminals within the operational range of the mobile base station. The Measurement Report function, used during handovers between base stations, is utilized for obtaining signal quality. Measurement Report is an RRC-layer feature in 5G communication.

Among the information obtained from the Measurement Report, this thesis uses RSRP as an indicator of signal strength. RSRP represents the received power of reference signals, which is influenced by the relative position of the terminal and the base station, as well as environmental factors such as base station deployment conditions and obstacles.

In this thesis, the goal is to improve signal quality among terminals by performing mobility control of the mobile base station based on the constructed Superimposed Signal Map, which consists of RSRP measurements at different locations.

The procedure for constructing the Superimposed Signal Map is as follows:

Step 1: Establish an SFTP connection to the compact PC serving as the base station and retrieve log files containing the RNTI and RSRP values of connected UEs. This initial log serves as a baseline for comparison in later steps.

Step 2: Wait for 5 seconds to allow for new signal measurements to be recorded.

Step 3: Retrieve the log file again and extract the differences by comparing it with the previously obtained log from Step 1. This allows us to capture any changes in signal strength.

Step 4: From the extracted differences, obtain RSRP values for each terminal. The average RSRP, variance, and position coordinates for each terminal over the 5-second measurement period are recorded.

Step 5: Move the mobile base station approximately 50 cm in the designated movement direction within the experimental environment, ensuring that signal variations across different locations are measured effectively.

This process is repeated iteratively until the total measurement duration, excluding movement time, reaches approximately 35 seconds. At the end of the measurement process, the mobile base station remains positioned at the final measurement location in the experimental environment.

2.2.2 Autonomous Mobility Control Based on the Superimposed Signal Map

To validate the proposed mobility control method for improving signal quality among terminals, an experimental system was implemented. Figure 3 illustrates an example of mobility control using the implemented system.

This mobility control aims to ensure that multiple terminals can communicate without degradation in signal quality through mobility control of the mobile base station. The core idea of the proposed method is to move the mobile base station toward terminals experiencing lower signal quality. The Measurement Report function, which is primarily used for base station handovers, is utilized to assess the communication quality of each terminal. Since Measurement Report is an RRC-layer feature in 5G communication, it provides real-time feedback on RSRP (Reference Signal Received Power), which is used as the primary metric for mobility control.

Based on the Signal Map constructed through radio environment sensing, the mobile

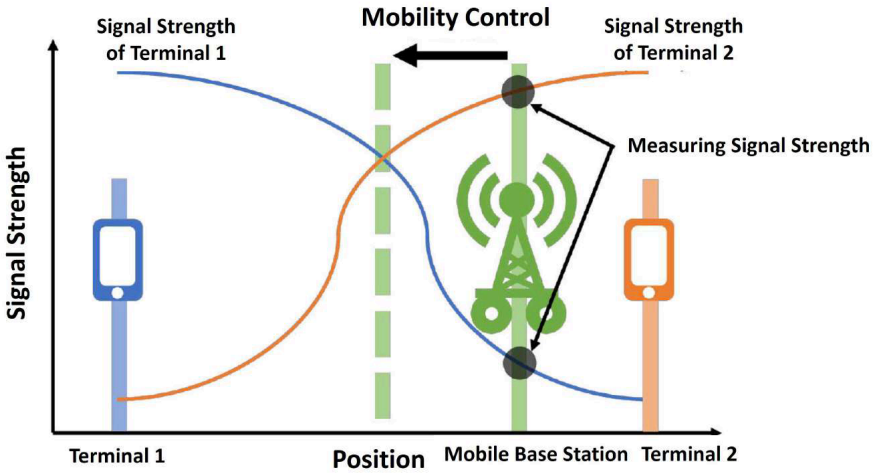

Figure 3: Conceptual Diagram of the Constructed System

base station autonomously determines its optimal position. The movement strategy is designed to maximize the average RSRP among multiple terminals while ensuring fairness in communication quality.

The autonomous mobility control method based on the Superimposed Signal Map follows these steps:

Step 1: Determine the target location where the average RSRP of two terminals is maximized based on the constructed Signal Map.

Step 2: Calculate the relative movement required to reach the target location from the current position.

Step 3: Instruct the mobile platform to move by the calculated movement amount, thereby executing mobility control to the target location.

After reaching the target location, RSRP measurements are performed again for 5 seconds. The average and variance of RSRP values over this period are computed for each terminal, allowing the system to reassess the signal quality and further refine mobility control in subsequent iterations.

2.2.3 Experimental Environment

This thesis aims to enable multiple terminals to communicate without signal quality degradation through mobility control of the mobile base station. To simplify the system, two

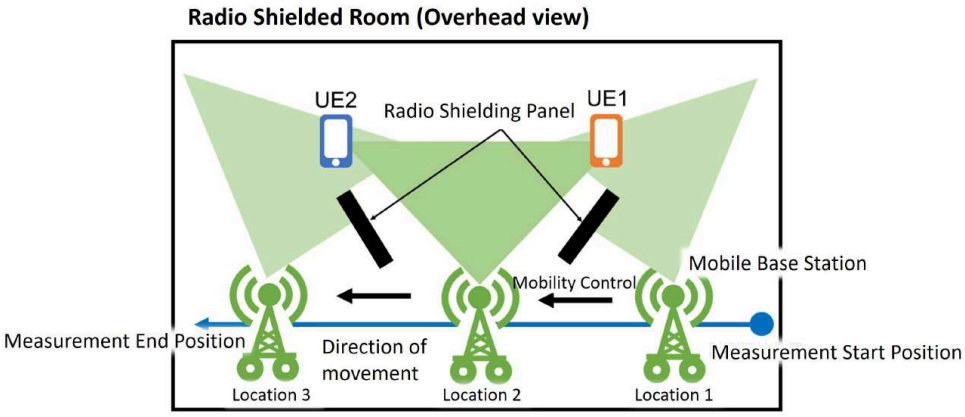

Figure 4: Experimental Environment Configuration

smartphones are used as terminals for validation. The terminals (UEs) connected to the 5G system are the Samsung Galaxy S21 5G and the Samsung Galaxy S21 Ultra 5G.

The experiments were conducted in a radio shielded room (Room 706, Graduate School of Information Science and Technology, Osaka University). The experimental environment was designed to create significant variations in signal quality at different locations due to obstacles. Multiple radio shielding panels were placed at specific positions inside the shielded room as obstacles.

As shown in Figure 4, panels were placed in front of each terminal to block signals from the mobile base station to one of the terminals, thereby creating differences in signal quality. Additionally, shielding panels were placed on the rear and side walls of the terminals to minimize the impact of signal reflection from the walls. At Location 1 and Location 2, the signal to one of the two terminals was blocked by a panel. In contrast, at Location 3, signals reached both terminals without obstruction. The objective of mobility control in this environment is to sense the radio environment while moving the mobile base station in a straight line, as indicated by the arrow in Figure 4, and to relocate the mobile base station near Location 3.

Photographs of the experimental environment taken at Locations 1, 2, and 3 are shown in Figures 5, 6, and 7.

Figure 5: Experimental Environment (Location 1)

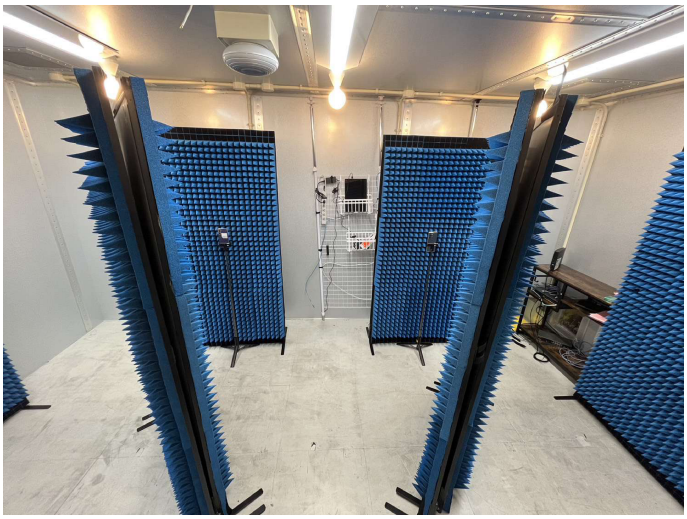

Figure 6: Experimental Environment (Location 2)

2.2.4 Evaluation Method

This thesis evaluates whether the mobility control method for mobile base stations, which utilizes the Measurement Report function used in handovers between base stations, can mitigate the cell-edge problem and allow multiple terminals to communicate without signal quality degradation.

In this experiment, the mobile base station autonomously moves to the location where the average RSRP of the two terminals is maximized, based on the Superimposed Signal

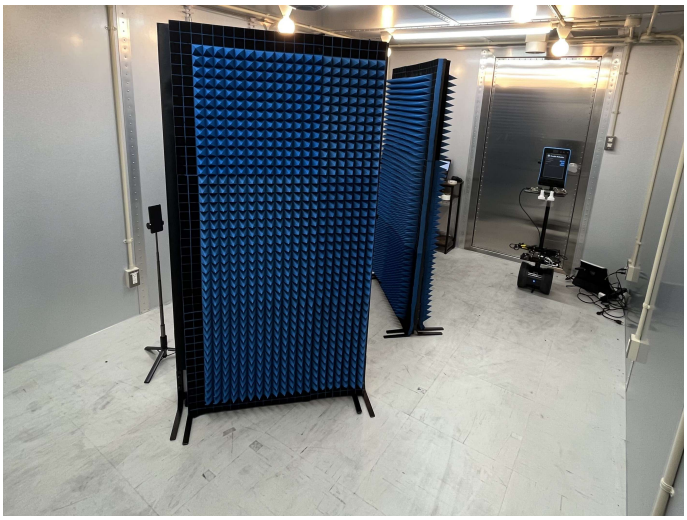

Figure 7: Experimental Environment (Location 3)

Map constructed through radio environment sensing.

The evaluation method consists of comparing the location where the average RSRP of the two terminals is maximized, as identified in the constructed Superimposed Signal Map, with the final position of the mobile base station after mobility control. The objective is to confirm whether these locations approximately match. Additionally, the signal strength of the two terminals before and after mobility control is compared.

Furthermore, the time-series variations of RSRP measured during the Superimposed Signal Map construction are presented for two different experimental environments.

2.2.5 Experimental Results

The Superimposed Signal Map obtained through radio environment sensing in the experimental environment is shown in Figure 8. Additionally, the time-series variations of RSRP during the map construction are presented in Figure 9. RSRP represents signal strength and is measured in dBm.

As a result of the experiment, at the initial measurement position where the distance from the starting point of the mobile base station was approximately 0m, the average RSRP of the two terminals was -116.9 dBm. Additionally, at the location where the mobile base station was positioned approximately 1.5m from the starting point, the average RSRP of the two terminals was maximized at -110.5 dBm. After executing mobility control, the

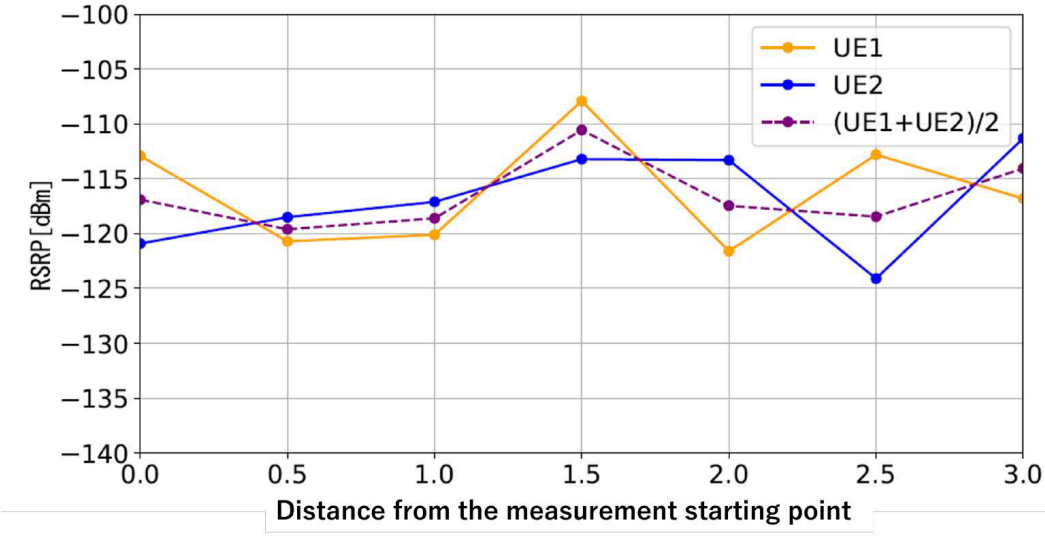

Figure 8: Constructed Superimposed Signal Map

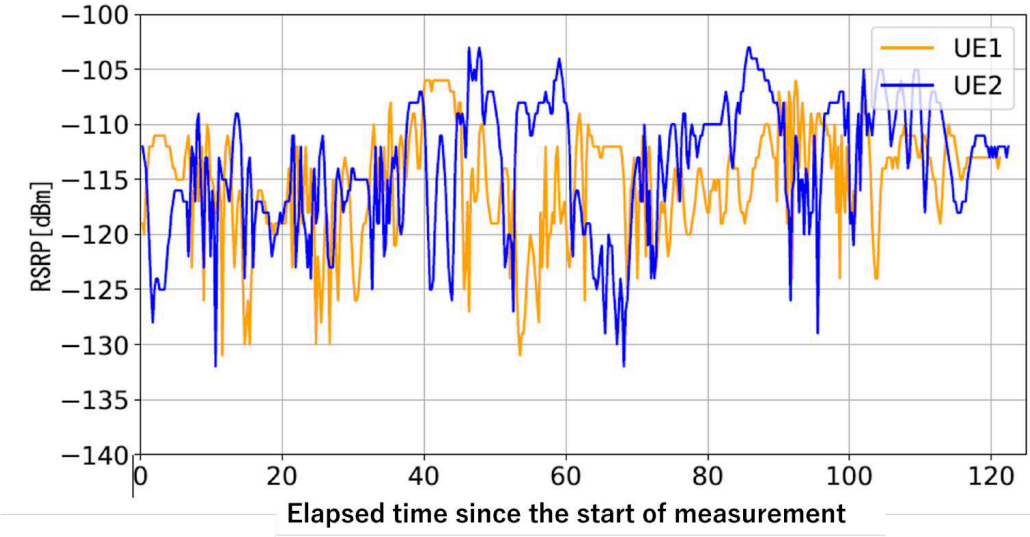

Figure 9: Time-Series Variations of RSRP

mobile base station moved to a position approximately 1.5m from the starting point, where the average RSRP of the two terminals was -112.5 dBm. The average RSRP across all measured locations was -116.5 dBm.

Table 4: Experimental Results

Distance from Starting Point [m]	0.0	0.5	1.0	1.5	2.0	2.5	3.0	Average
RSRP[dBm] (Average Value)	-116.9	-119.6	-118.6	-110.5	-117.5	-118.5	-114.0	-116.5

These results confirm that autonomous mobility control of the mobile base station is feasible using the Superimposed Signal Map constructed through radio environment sensing with the Measurement Report function. Specifically, in an environment where obstacles exist and there is significant signal quality variation at different locations, the proposed mobility control method effectively positions the mobile base station at the location where the sum of the RSRP values of the two terminals is maximized. Additionally, since the RSRP at the location after mobility control is higher than both the initial RSRP at the experiment's starting position and the average RSRP across all locations, it is confirmed that mobility control of the mobile base station improves the communication quality of both terminals.

2.2.6 Necessity of Two-Dimensional and Three-Dimensional Superimposed Signal Map Construction

In this experiment, the measurement of the radio environment was limited to one-dimensional linear movement of the mobile base station. However, for practical deployment, a more comprehensive understanding of the radio environment is essential. Constructing two-dimensional and three-dimensional Superimposed Signal Maps is crucial for optimizing base station placement and improving mobility control.

In urban and indoor environments, radio waves are significantly attenuated and reflected by buildings and obstacles. These effects make it difficult to determine an optimal base station placement using only linear movement. By enabling the mobile base station to conduct measurements from multiple directions, a more precise estimation of the radio environment can be achieved. However, increasing the number of measurement points leads to higher costs and computational complexity, requiring an efficient method for reconstructing the signal distribution from sparse observations. Additionally, in high-frequency

5G bands, the impact of height (Z-axis) is significant. Elevation differences—such as between floors in a building or UAV (drone)-based base stations—must be considered. In multi-floor indoor environments and high-rise buildings, millimeter-wave propagation is highly complex, making mobility control particularly challenging.

Traditional base station deployment relies on large-scale radio propagation simulations that optimize network coverage and throughput over long timescales. These methods assume fixed infrastructure and focus on maximizing network-wide efficiency. However, mobile base stations differ fundamentally in their objective: instead of expanding coverage, they must maintain stable communication quality for moving or unknown-position terminals in real time. Conventional simulation-based approaches are ineffective in such scenarios, as they do not account for rapid environmental fluctuations or dynamic terminal locations. Moreover, directly measuring radio wave conditions across an entire area is impractical due to time and resource constraints. Instead, an estimation technique is needed to reconstruct two-dimensional and three-dimensional radio distributions from limited measurement data.

To address these challenges, this thesis introduces a Superimposed Signal Map estimation method using Bayesian Compressive Sensing (BCS). BCS reconstructs the radio environment with minimal observation points, allowing the mobile base station to dynamically adjust its position while ensuring fair communication quality among multiple terminals. A key challenge in this approach is ensuring that the mobile base station continuously adapts its position to real-time changes in the radio environment while maintaining stable communication quality. Unlike static network optimization, where base stations are fixed and extensive pre-measurements can be conducted, mobile base stations operate under constantly changing conditions, requiring continuous updates to the signal map.

Since the primary objective is to dynamically adjust the base station's position to ensure stable communication quality for terminals, conventional prediction methods based on static propagation models are insufficient. These models optimize long-term network performance but do not effectively adapt to short-term environmental variations. Therefore, an effective mobility control system must integrate efficient sparse data collection, signal estimation, and real-time decision-making to optimize base station placement in two-dimensional and three-dimensional environments.

3 Wireless Signal Mapping and Mobility Control Methods for Mobile Base Stations

3.1 A Concept of Superimposed Signal Map

The Superimposed Signal Map (SSM) represents the average signal quality of all terminals with respect to the mobile base station, obtained at each position of the mobile base station and projected onto a spatial grid. By constructing the SSM, it becomes possible to assess overall communication quality and determine appropriate base station positions for improved fairness and stability.

Figure 10 illustrates an example of the SSM concept with two terminals. The signal strength received from Terminal1 and Terminal2 varies depending on their relative positions to the mobile base station. Each terminal's received signal strength (RSRP) is represented as a spatial distribution, and the SSM is formed by averaging these values across the entire grid. This allows the system to estimate signal quality in unobserved regions and guide the movement of the mobile base station.

Unlike conventional static base station placement, which optimizes coverage based on pre-measured models, the SSM enables dynamic adaptation to environmental changes by estimating signal quality across different locations. In 5G and beyond networks, where high-frequency signals are sensitive to obstructions, precise base station positioning is essential.

Since direct measurement of all locations is impractical, the SSM employs Bayesian Compressive Sensing (BCS) to estimate the signal distribution from limited observations. This thesis utilizes the SSM to develop a mobility control system that dynamically adjusts the mobile base station's position based on real-time signal quality, ensuring fair communication among multiple terminals.

3.2 Overview of Mobility Control Method

In this thesis, we propose a method that utilizes a mobile base station to efficiently construct a Superimposed Signal Map representing the signal strength of multiple terminals at each location within an area and controls the movement of the mobile base station to

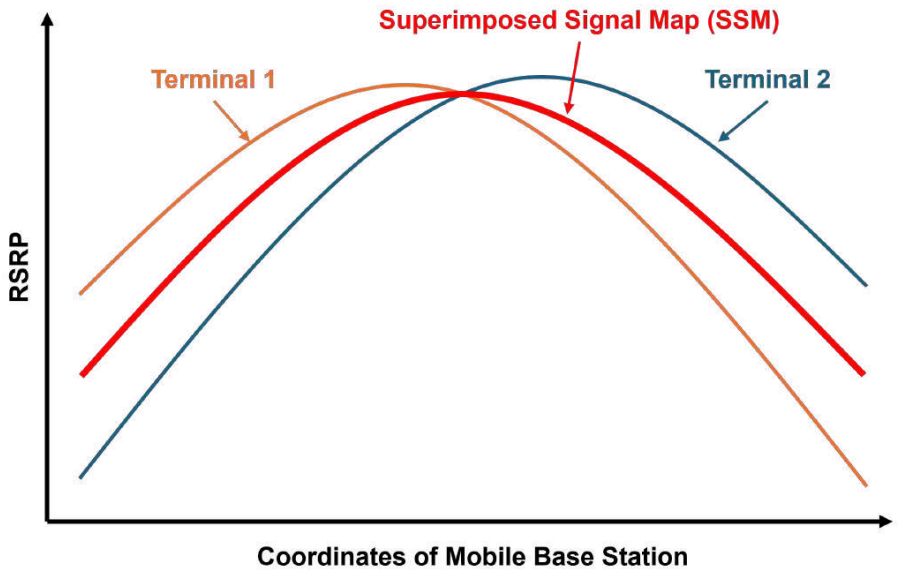

Figure 10: Concept of the Superimposed Signal Map (SSM) with Two Terminals. The individual RSRP distributions from Terminal1 and Terminal2 are combined to form the SSM, which represents the average RSRP at each position.

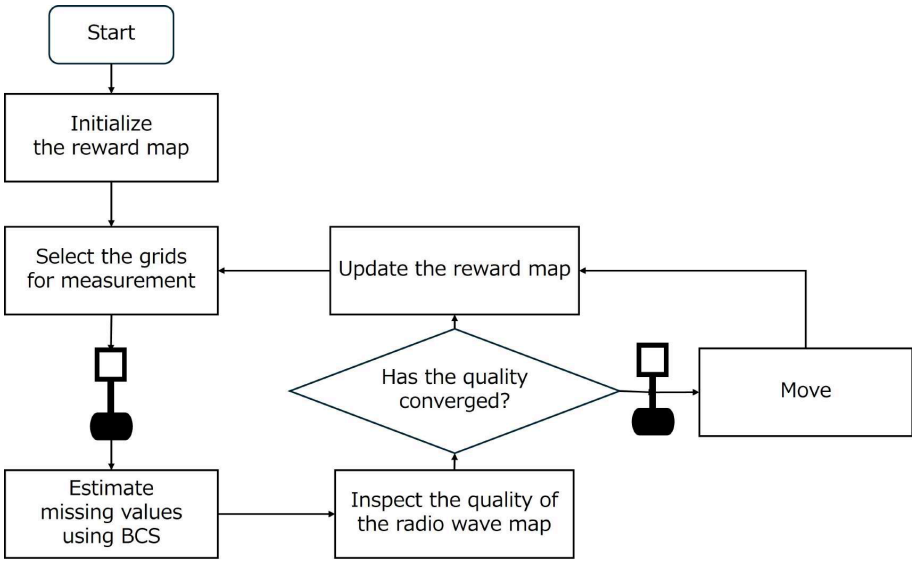

Figure 11: Mobility Control Method for the Mobile Base Station

a position where signal quality is balanced among terminals (Figure 11).

In indoor environments with numerous obstacles, it is impractical to densely observe all

regions. Therefore, it is necessary to estimate the signal strength in unobserved areas, even when observation data is sparse. To address this challenge, this thesis employs Bayesian Compressive Sensing (BCS). BCS is an algorithm that efficiently estimates unobserved signal values based on sparse signal observation data. It also provides confidence intervals for the estimated values, enabling both efficient observation and reliable estimation.

The basic flow of the method is as follows:

First, the mobile base station initializes the reward map. Since no measurements have been conducted at this stage, the initial reward values are assigned randomly. Once the reward map is initialized, the mobile base station begins measuring signal strength at its initial location.

The area is then divided into a grid of fixed size, and the reward map is updated based on the measurement data. The reward map assigns higher rewards to grid cells where radio wave distribution uncertainty is high and mobility costs are low. The mobile base station selects the grid cell with the highest reward for its next movement.

Next, the mobile base station moves to the selected grid cell and measures the signal strength received by smartphones currently communicating within the area. The measured data is used to record the spatial distribution of signal strength. Once measurements are completed, BCS is applied to estimate the overall signal distribution across the area, including unobserved regions. This estimation process enables the reconstruction of a Superimposed Signal Map covering the entire area.

Based on the estimated Superimposed Signal Map, the optimal location where the average signal strength among multiple terminals is maximized is calculated. This calculation aims to improve the average signal strength for all smartphones based on the estimated Superimposed Signal Map, determining the next position to which the mobile base station should move.

Finally, the mobile base station moves to the calculated position and provides communication services to the terminals. This process is iterated until the uncertainty of the estimated Superimposed Signal Map falls below a predefined threshold.

While the proposed method enables the mobile base station to improve communication quality by adjusting its position, a key challenge lies in estimating signal strength across unobserved locations using a limited number of measurements. Since measuring all grid

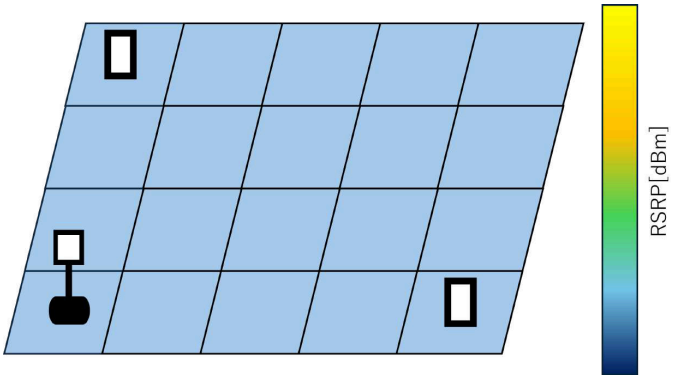

Figure 12: Superimposed Signal Map at time $t-1$. Each grid contains: $\boldsymbol{f}_{t-1}^{n} = \left(\left[L_x^n, L_y^n\right], x_{t-1}^n\right)$

.

points directly is impractical due to time and resource constraints, an estimation method that can reconstruct the signal distribution from sparse observations is necessary.

To achieve this, we employ Bayesian Compressive Sensing (BCS), which enables efficient estimation of the Superimposed Signal Map with minimal sampling while incorporating uncertainty quantification. The following section details the application of BCS for signal estimation and its integration into the mobility control framework.

3.3 Bayesian Compressive Sensing for Radio Signal Estimation

In signal prediction using BCS, the target area is divided into N grid cells, and the signal data x for all N grid cells is predicted based on the samples y obtained from M grid cells and the projection matrix Φ [11, 12].

At time $t-1$, the signal at the n-th RP is given by:

$$\boldsymbol{f}_{t-1}^{n} = \left(\left[L_x^n, L_y^n\right], x_{t-1}^n\right), \tag{1}$$

where x_{t-1}^n represents the RSSI at that RP (Figure 12).

The overall signal strength represented by the Superimposed Signal Map is expressed as:

$$\boldsymbol{x}_{t-1} = \left[x_{t-1}^1, \ldots, x_{t-1}^N\right]^T. \tag{2}$$

The N-dimensional vector representing all signal changes at N RPs from $t-1$ to t is

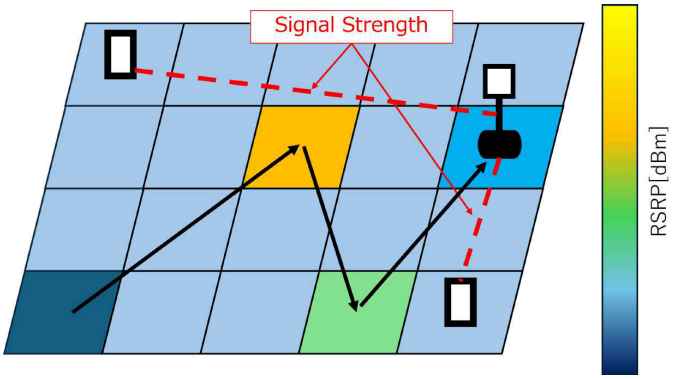

Figure 13: Measured grids (sample grids)

given by:

$$\boldsymbol{\Delta x}_t = \boldsymbol{x}_t - \boldsymbol{x}_{t-1}, \tag{3}$$

where

$$\boldsymbol{\Delta x}_t = \left[\Delta x_t^1, \ldots, \Delta x_t^N\right]^T. \tag{4}$$

The goal of the Superimposed Signal Map reconstruction problem is to estimate $\boldsymbol{\Delta x}_t$.

In the reconstruction phase, new samples are measured and aggregated from time $t-1$ to t (Figure 13). Each new sample is first mapped onto the grid where the measurement was taken. When multiple new measurement samples are mapped to the same grid, their signal strengths are averaged and stored for that grid. Subsequently, new samples are mapped to M different grids, forming M sample grids. Each sample grid contains a new signal sample y_t^m.

Specifically, similar to $\boldsymbol{f}_{t-1}^n$, the m-th sample grid at time t is given by:

$$\widetilde{\boldsymbol{f}}_t^m = \left(\left[\widetilde{L}_x^m, \widetilde{L}_y^m\right], y_t^m\right), \tag{5}$$

where the coordinates $\left[\widetilde{L}_x^m, \widetilde{L}_y^m\right]$ represent the center position of the grid on the map. The measured signal strength at the M sample grids is expressed as:

$$\boldsymbol{y}_t = \left[y_t^1, \ldots, y_t^M\right]^T. \tag{6}$$

The change in signal strength at the m-th sample grid is calculated as the difference between the newly measured sample y_t^m at time t and the past signal strength $\widetilde{x}_{t-1} \in \boldsymbol{x}_{t-1}$ at the nearest RP in the previous Superimposed Signal Map. That is,

$$\Delta y_t^m = y_t^m - \widetilde{x}_{t-1}. \tag{7}$$

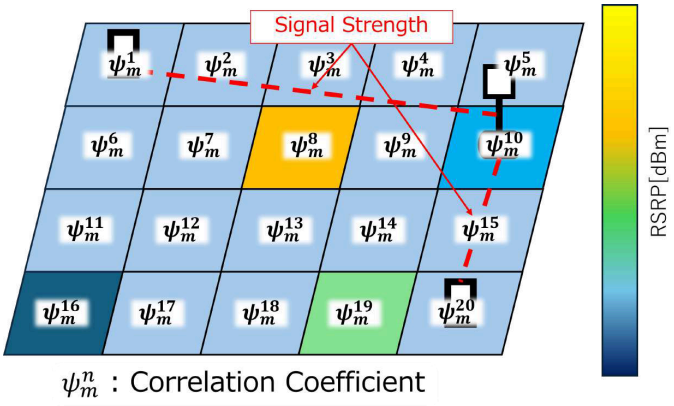

Figure 14: Correlation coefficients between sample grids and all other grids

The vector $\boldsymbol{\Delta y}_t \in \mathbb{R}^M$ represents all measured signal strength changes at the M sample grids, given by:

$$\boldsymbol{\Delta y}_t = \left[\Delta y_t^1, \ldots, \Delta y_t^M\right]^T, \tag{8}$$

where $\boldsymbol{\Delta y}_t$ is subject to measurement noise $e_m \sim \mathcal{N}\left(0, \sigma^2\right)$.

Given the previous signal map $\boldsymbol{x}_{t-1}$ and sparsely measured samples $\boldsymbol{y}_t$, we first determine the signal changes $\boldsymbol{\Delta y}_t$ observed at the sample grids. Then, in the reconstruction phase, we estimate the complete signal changes $\boldsymbol{\Delta x}_t$ based on these sparse $\boldsymbol{\Delta y}_t$. The key challenge in signal map reconstruction is determining $\boldsymbol{\Delta x}_t$ given only $\boldsymbol{\Delta y}_t$.

Each individual crowd-sourced signal change Δy_t^m can be formulated as a partial sample from the complete signal change $\boldsymbol{\Delta x}_t$. To recover the full Superimposed Signal Map from these sparse samples, BCS is employed.

Specifically, for each sample grid $\widetilde{f_t^m}$, correlations with all other grids in the area are computed (Figure 14). Let ψ_m^n denote the sensing coefficient between the measured signal change Δy_t^m and the n-th complete signal change Δx_t^n. The relationship between each measured signal change Δy_t^m and the overall signal change $\boldsymbol{\Delta x}_t$ is expressed as:

$$\Delta y_t^m = \boldsymbol{\psi}_m \boldsymbol{\Delta x}_t + e_m, \tag{9}$$

where

$$\boldsymbol{\psi}_m = \left[\psi_m^1, \psi_m^2, \ldots, \psi_m^n, \ldots, \psi_m^N\right] \tag{10}$$

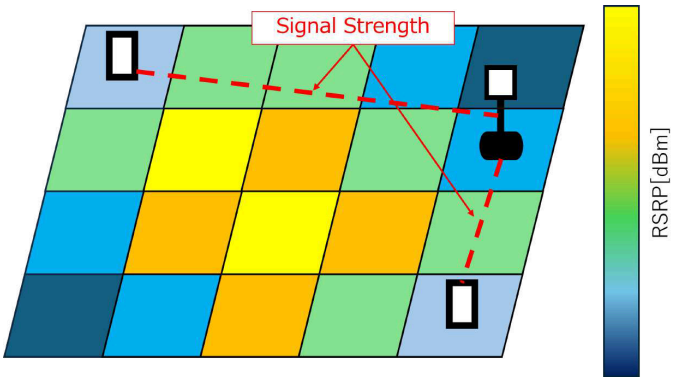

Figure 15: Estimated Superimposed Signal Map at time t

and

$$\sum_{n=1}^{N} \psi_m^n = 1, \quad 0 \leq \psi_m^n \leq 1. \tag{11}$$

This indicates that the measured signal change is a weighted sum of the complete signal changes at all RPs. A larger ψ_m^n value implies that the measured signal change is closer to the n-th RP and has a higher likelihood of being correlated with that signal.

Let $\mathbf{e}_{M\times 1} = [e_1, \ldots, e_m, \ldots, e_M]^T$. Summarizing the relationship between the M measured signal changes $\boldsymbol{\Delta y}_t$ and the complete signal changes $\boldsymbol{\Delta x}_t$, we obtain the following overall subsampling equation:

$$(\boldsymbol{\Delta y}_t)_{M\times 1} = \boldsymbol{\Phi}_{M\times N} (\boldsymbol{\Delta x}_t)_{N\times 1} + \boldsymbol{e}_{M\times 1}, \tag{12}$$

where the sensing matrix Φ is given by:

$$\boldsymbol{\Phi} = [\boldsymbol{\psi}_1, \boldsymbol{\psi}_2, \ldots, \boldsymbol{\psi}_m, \ldots, \boldsymbol{\psi}_M]^\top. \tag{13}$$

Ultimately, the signal map reconstruction problem is to determine $\boldsymbol{\Delta x}_t$ given $\boldsymbol{\Delta y}_t$ and $\boldsymbol{\Phi}$ in Equation (12). Once the complete signal change is obtained, the full Superimposed Signal Map $\boldsymbol{x}_t$ is constructed as follows:

$$\boldsymbol{x}_t = \boldsymbol{x}_{t-1} + \boldsymbol{\Delta x}_t \tag{14}$$

(Figure 15).

3.3.1 Solution Method for Bayesian Compressive Sensing (BCS)

We describe a method to estimate the posterior distribution $p(\boldsymbol{\Delta x}_t)$ based on the prior distributions of the measured signal change $\boldsymbol{\Delta y}_t$, $\boldsymbol{\Delta x}_t$, and σ^2. Let α_n be the inverse of $\left(\sigma_{t-1}^n\right)^2 + (\sigma_t^n)^2$, and define:

$$\boldsymbol{\alpha} = [\alpha_1, \ldots, \alpha_n]. \tag{15}$$

Given that $\Delta x_t^n \sim \mathcal{N}\left(\Delta \bar{x}_t, (\sigma_{t-1}^n)^2\right)$, the prior distribution is:

$$p(\boldsymbol{\Delta x}_t \mid \boldsymbol{\alpha}) = \prod_{n=1}^{N} \mathcal{N}\left(\Delta \bar{x}_t, \alpha_n^{-1}\right). \tag{16}$$

Let β be the precision of the noise $\boldsymbol{e}$ (i.e., $\beta = \sigma^{-2}$). The initial values of $\boldsymbol{\Delta x}_0$ and β can be extracted from the initial version of the signal map at time 0 or defined using a general hierarchical prior distribution.

Given the measured signal change $\boldsymbol{\Delta y}_t$, the posterior distribution of $\boldsymbol{\Delta x}_t$, along with parameters $\boldsymbol{\alpha}$ and β, is expressed as:

$$p(\boldsymbol{\Delta x}_t, \boldsymbol{\alpha}, \beta \mid \boldsymbol{\Delta y}_t) = p(\boldsymbol{\Delta x}_t \mid \boldsymbol{\alpha}, \beta, \boldsymbol{\Delta y}_t)\, p(\boldsymbol{\alpha}, \beta \mid \boldsymbol{\Delta y}_t). \tag{17}$$

In the above equation, the posterior distribution $p(\boldsymbol{\Delta x}_t \mid \boldsymbol{\alpha}, \beta, \boldsymbol{\Delta y}_t)$ can be computed analytically:

$$p(\boldsymbol{\Delta x}_t \mid \boldsymbol{\alpha}, \beta, \boldsymbol{\Delta y}_t) = (2\pi)^{-\frac{N}{2}} |\boldsymbol{\Sigma}|^{-\frac{1}{2}} \exp\left(-\frac{1}{2}(\boldsymbol{\Delta x}_t - \boldsymbol{\mu})^\top \boldsymbol{\Sigma}^{-1} (\boldsymbol{\Delta x}_t - \boldsymbol{\mu})\right), \tag{18}$$

where the posterior mean $\boldsymbol{\mu}$ and covariance $\boldsymbol{\Sigma}$ are given by:

$$\boldsymbol{\mu} = \beta \boldsymbol{\Sigma} \boldsymbol{\Phi}^\top \boldsymbol{\Delta y}_t, \quad \boldsymbol{\Sigma} = \left(\beta \boldsymbol{\Phi}^\top \boldsymbol{\Phi} + \boldsymbol{A}\right)^{-1}, \tag{19}$$

where $\boldsymbol{A} = \operatorname{diag}(\alpha_1, \alpha_2, \ldots, \alpha_n, \ldots, \alpha_N)$.

Since $\boldsymbol{\mu}$ and $\boldsymbol{\Sigma}$ depend on parameters $\boldsymbol{\alpha}$ and β, it is necessary to determine $\boldsymbol{\alpha}$ and β to maximize the posterior distribution $p(\boldsymbol{\alpha}, \beta \mid \boldsymbol{\Delta y}_t)$.

To estimate these parameters, we apply Type-II Maximum Likelihood (ML-II) estimation [13]. Let Σ_{nn} be the n-th diagonal element of $\boldsymbol{\Sigma}$, representing the variance of the n-th signal RSSI change. The updated α_n^{new} is given by:

$$\alpha_n^{\text{new}} = \frac{1 - \alpha_n \Sigma_{nn}}{\mu_n^2}, \quad n \in \{1, 2, \ldots, N\}, \tag{20}$$

where μ_n is the n-th element of the vector $\boldsymbol{\mu}$. Similarly, the updated β^{new} is given by:

$$\beta^{\text{new}} = \frac{M - \text{Tr}(\boldsymbol{I} - \boldsymbol{A}\boldsymbol{\Sigma})}{\|\boldsymbol{\Delta}\boldsymbol{y}_t - \boldsymbol{\Phi}\boldsymbol{\mu}\|_2^2}, \tag{21}$$

where $\text{Tr}(\boldsymbol{A})$ is the trace (sum of diagonal elements) of matrix $\boldsymbol{A}$.

Given initial values of $\boldsymbol{\alpha}$ and β, the values of $\boldsymbol{\mu}$ and $\boldsymbol{\Sigma}$ are computed iteratively based on the above equations and updated in subsequent iterations.

3.4 Reward Map Definition

This section describes the reward map, which serves as the criterion for selecting the grid to be measured by the mobile base station.

In previous studies on crowdsourced Superimposed Signal Map construction [11], models have been proposed where multiple users perform discrete measurements at different locations. In contrast, this thesis focuses on a single mobile base station that performs measurements while moving. Therefore, to optimize movement and measurement efficiency, it is necessary to incorporate information obtained during movement into the decision-making process.

To evaluate the overall movement path, the total reward R_p is defined as follows:

$$R_p = \sum_{j \in p} \frac{\sigma_j^2}{c(i,j)^\lambda}, \tag{22}$$

where:

- R_p: Total reward for path p.
- $j \in p$: Each location on path p.
- σ_j^2: Uncertainty at location j (variance of the signal strength prediction distribution).
- $c(i,j)$: Movement cost from the current location i to location j.
- λ: Parameter that determines the influence of distance from the current location on the reward.

This model normalizes the amount of uncertainty reduction at each location j by the movement cost $c(i,j)$, enabling efficient exploration. The optimal movement path p^* is

then defined as:

$$p^* = \arg\max_p (R_p). \tag{23}$$

To ensure efficient data collection, the model selects 10 measurement locations per sampling iteration, optimizing the balance between uncertainty reduction and movement cost.

This approach allows for an exploration strategy that maximizes efficiency over the entire movement path. Additionally, the model is designed to prioritize paths that traverse areas with a high proportion of uncertainty rather than being biased toward a single high-uncertainty location.

3.4.1 Conditions for Terminating Measurement and Post-Termination Movement

To ensure efficient data collection, the mobile base station must have defined conditions for continuing and stopping measurements. Measurements are terminated when one of the following conditions is met. First, when the average uncertainty σ_j^2 across all grids falls below a predefined threshold ϵ, it indicates that sufficient signal quality data has been collected, allowing the measurement process to conclude. Second, when the elapsed time since the start of measurement exceeds the predefined maximum measurement time $T_{\max}$, the system halts further measurements to prevent excessive resource consumption.

Once measurements are stopped, the mobile base station determines the optimal movement destination. Based on the collected data, it predicts the location where the average of signal strengths from multiple smartphones is maximized and moves to that position to improve overall communication quality.

3.4.2 Methods for Reducing Computational Complexity

The onboard computer of the mobile base station is assumed to have limited processing power, and since the base station operates over extended periods, power efficiency is crucial. Thus, calculating rewards for all possible paths is impractical.

To address this, the search space is constrained by evaluating only a set of candidate locations $\mathcal{N}(i)$ within a predefined search radius $D_{\max}$, reducing both computational complexity and movement cost:

$$\mathcal{N}(i) = \{j \mid d(i,j) \leq D_{\max}\}. \tag{24}$$

3.4.3 Measurement of Signal Quality

In this thesis, the Measurement Report function is used to measure signal quality [14, 15]. Measurement Report is an RRC (Radio Resource Control) layer feature in 5G communication, primarily used for handovers [16].

While it is possible to acquire signal quality with shorter intervals using CSI information or OFDM signal processing data, these methods introduce additional computational complexity, increased power consumption, and additional hardware weight. Therefore, this thesis utilizes the Measurement Report function to obtain RSRP.

4 Evaluation

This section provides a detailed description of the simulation environment and configurations used to validate the proposed method. The simulations are conducted using MATLAB.

4.1 Environment Configuration

The simulation environment is based on an outdoor area surrounding the Graduate School of Information Science and Technology at Osaka University (Figures 16 and 17). The environment size is approximately 100m × 100m, divided into 400 grid cells of 5m × 5m. The center of each grid is considered a measurement point for the mobile base station.

4.2 Data Generation

To generate a Superimposed Signal Map representing the average RSRP for n fixed smartphones at each location within the area, a radio wave simulator is employed. The simulator provides realistic signal propagation data, which serves as the dataset for this thesis. The base station's transmission power is set to 36.6 dBm.

Red dots in the figures indicate the locations of the smartphones used in the simulation. Yellow star markers represent the locations where the RSRP is at its maximum value. For terminals that cannot establish a connection with the base station due to obstacles or distance, the RSRP is generated as -250 dBm to represent the absence of a viable signal.

Since the penetration rate of radio waves in indoor environments is not accurately modeled in the simulator, indoor data points are excluded from the analysis. As a result, a total of 283 outdoor data points are used for further evaluation.

Figure 18 and Figure 19 show the Superimposed Signal Maps generated by the radio wave simulator for cases where the number of smartphones is 2 and 3, respectively.

4.3 Evaluation Metrics

To assess the effectiveness of the proposed method, the primary evaluation metric used is the **Communication Quality Improvement Rate**, which measures the enhancement in the average Reference Signal Received Power (RSRP) across multiple devices before

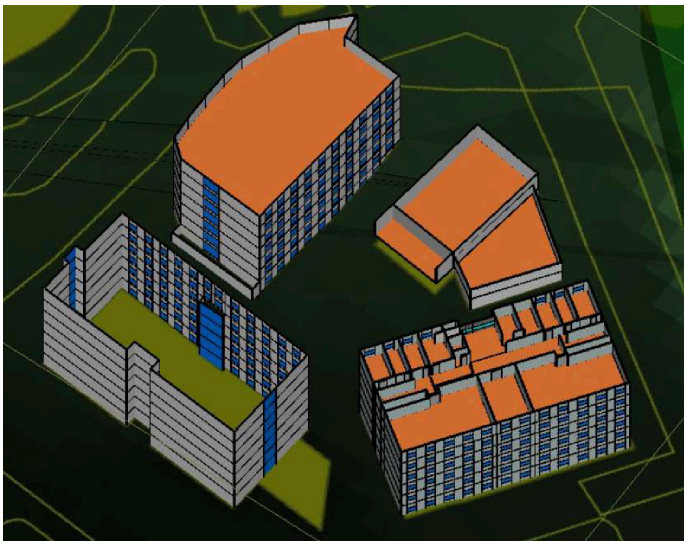

Figure 16: Simulation Environment: Outdoor Area of Osaka University (3D View)

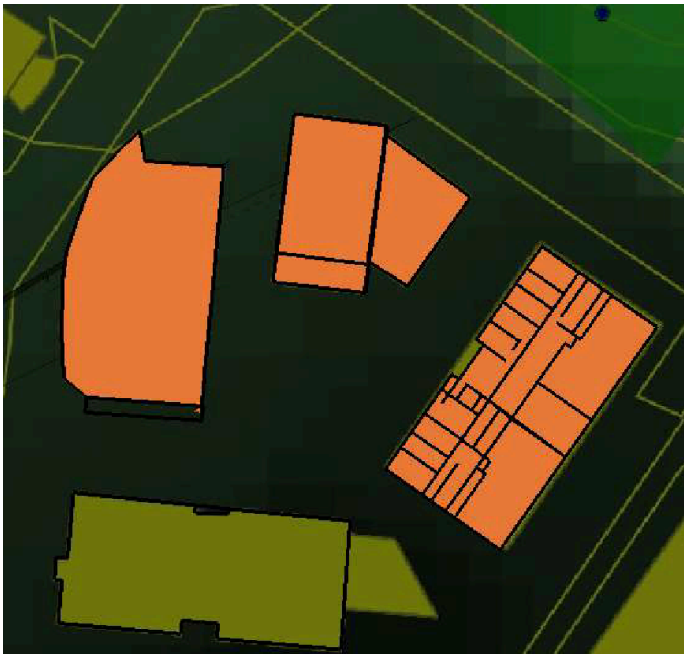

Figure 17: Simulation Environment: Outdoor Area of Osaka University (2D View)

and after mobility control. This metric assesses the extent to which the proposed method optimizes the placement of the mobile base station to achieve a balanced and improved signal distribution among devices. The improvement is calculated by comparing the average RSRP values of n smartphones before and after the mobility control process.

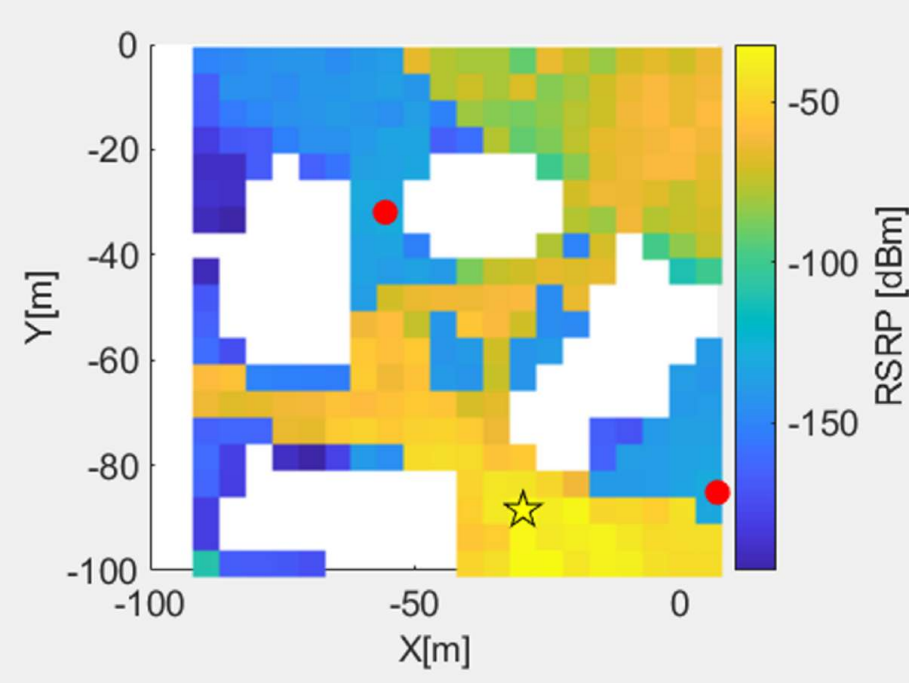

Figure 18: Ground-truth Superimposed Signal Map for 2 Devices generated by the radio wave simulator

Additionally, the effectiveness of the method is further analyzed through visual representations, including the Superimposed Signal Map, Uncertainty Map, and comparisons of ground-truth and predicted RSRP values. These visualizations provide insights into how well the mobility control algorithm minimizes uncertainty and improves signal strength distribution across the network.

4.4 Simulation Setup

The simulation is conducted following these steps.

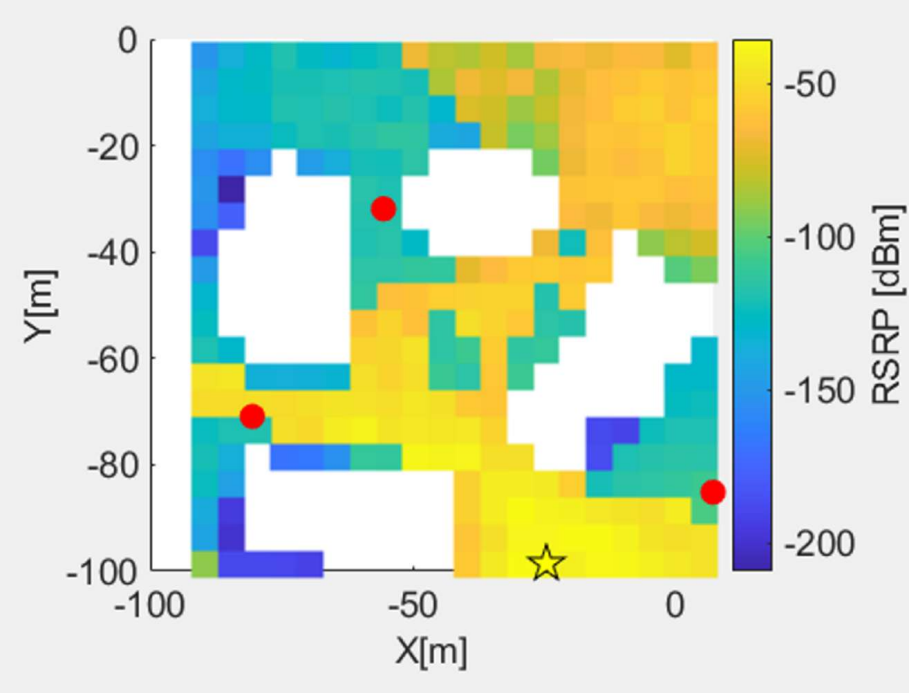

Figure 19: Ground-truth Superimposed Signal Map for three devices generated by the radio wave simulator

Step 1: Signal strength data for n fixed smartphones is generated using a radio wave simulator.

Step 2: The mobile base station moves within the area and periodically measures signal strength at each grid.

Step 3: Bayesian Compressive Sensing (BCS) is applied to construct the Superimposed Signal Map from the collected measurements.

Step 4: The movement of the mobile base station is controlled based on the computed optimal path, ensuring balanced communication quality among n smartphones.

Step 5: The effectiveness of the proposed method is evaluated based on the defined evaluation metrics.

The simulation is conducted under specific constraints. The maximum movement distance per iteration, D_{MAX}, is set to 10. Each sampling process selects 10 measurement points, and the threshold parameter ϵ is set to 1.0.

Table 5: Improvement in RSRP After Mobility Control (Two Devices)

Terminal	RSRP [dBm]	
	Before Mobility Control	After Mobility Control
Terminal 1	-84.375	-58.050
Terminal 2	-250.000	-54.871
Average RSRP	-167.188	-56.461
Overall Improvement [dBm]	110.727	

Table 6: Improvement in RSRP After Mobility Control (Three Devices)

Terminal	RSRP [dBm]	
	Before Mobility Control	After Mobility Control
Terminal 1	-84.375	-54.296
Terminal 2	-250.000	-52.217
Terminal 3	-74.871	-60.087
Average RSRP	-136.415	-55.533
Overall Improvement [dBm]	80.882	

4.5 Evaluation Results

The primary objective of this evaluation is to quantify how much the RSRP (Reference Signal Received Power) of each terminal improves before and after mobility control. Tables 5 and 6 present the key results for two and three devices, respectively, focusing on the average RSRP values before and after mobility control.

For the two-device case, the uncertainty map converged after 7 iterations, meaning that a total of 70 locations were sampled. Similarly, for the three-device case, uncertainty convergence was achieved after 12 iterations, resulting in 120 sampled locations. These results confirm that the proposed method efficiently optimizes the measurement process and ensures a balanced improvement in communication quality.

Tables 5 and 6 present the key results for two and three devices, respectively, focusing on the average RSRP values before and after mobility control.

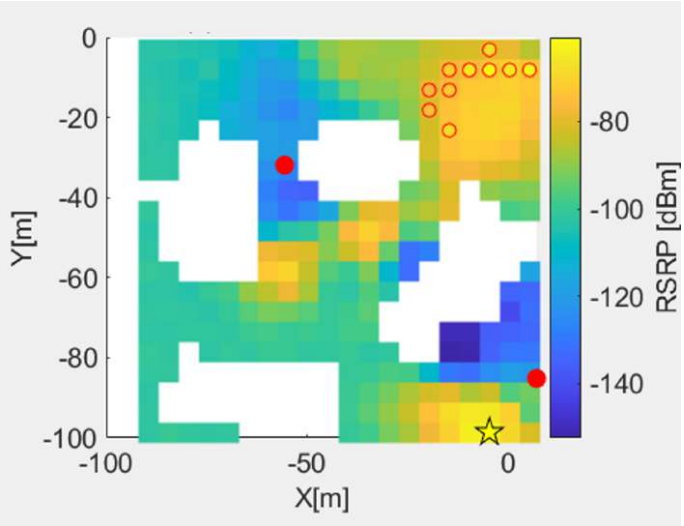

Figure 20: Predicted Superimposed Signal Map After Mobility Control (Two Devices). The yellow star indicates the estimated maximum RSRP location, where the mobile base station has moved. Red filled circles represent the device positions, and red outlined circles denote the sampled locations.

4.5.1 RSRP Analysis

The results in Tables 5 and 6 demonstrate that the mobility control significantly improved the communication quality of each terminal.

In the two-device case, the average RSRP improved from -167.188 dBm to -56.461 dBm, resulting in an overall improvement of 110.727 dB. Similarly, in the three-device case, the average RSRP increased from -136.415 dBm to -55.533 dBm, corresponding to an overall improvement of 80.882 dB. Furthermore, the weakest terminal in both cases experienced an improvement of at least 80.000 dBm, reducing communication disparities and ensuring a more balanced signal distribution among the terminals.

4.5.2 Visual Representation of Improvement

Figures 20 and 22 illustrate the predicted Superimposed Signal Map (SSM) after mobility control for two and three devices, respectively. These figures depict the estimated RSRP distribution after the mobile base station has completed measurement and prediction. The yellow star marks the estimated maximum RSRP location, where the mobile base station

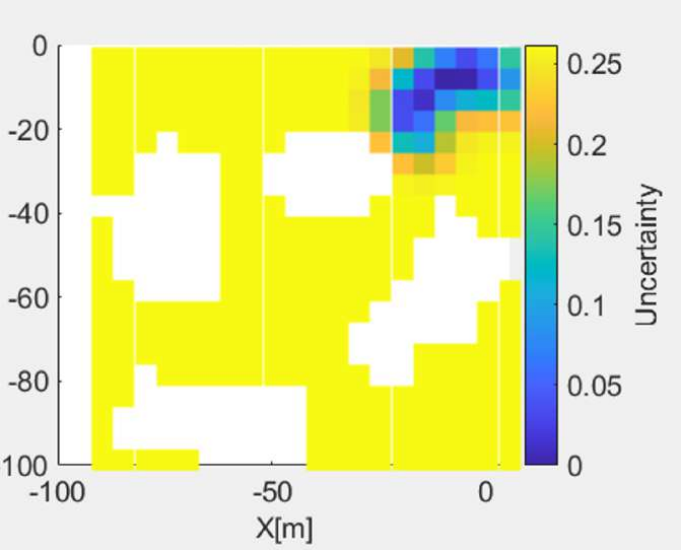

Figure 21: Uncertainty Map After Mobility Control (Two Devices). Darker areas indicate reduced uncertainty following the sampling process.

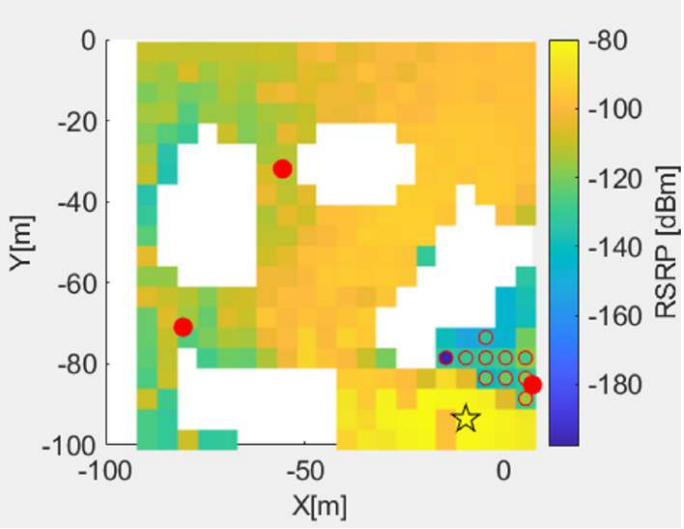

Figure 22: Predicted Superimposed Signal Map After Mobility Control (Three Devices). The yellow star indicates the estimated maximum RSRP location, where the mobile base station has moved. Red filled circles represent the device positions, and red outlined circles denote the sampled locations.

has ultimately moved. The red filled circles indicate the positions of the devices, while the red outlined circles represent the locations where sampling was performed.

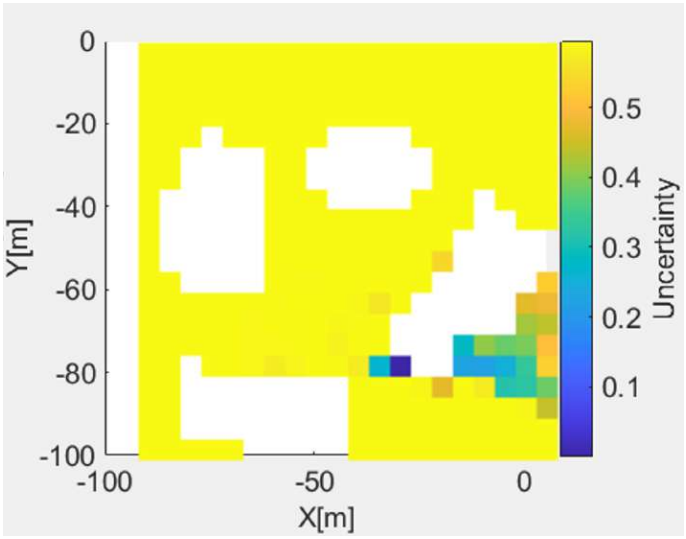

Figure 23: Uncertainty Map After Mobility Control (Three Devices). Darker areas indicate reduced uncertainty following the sampling process.

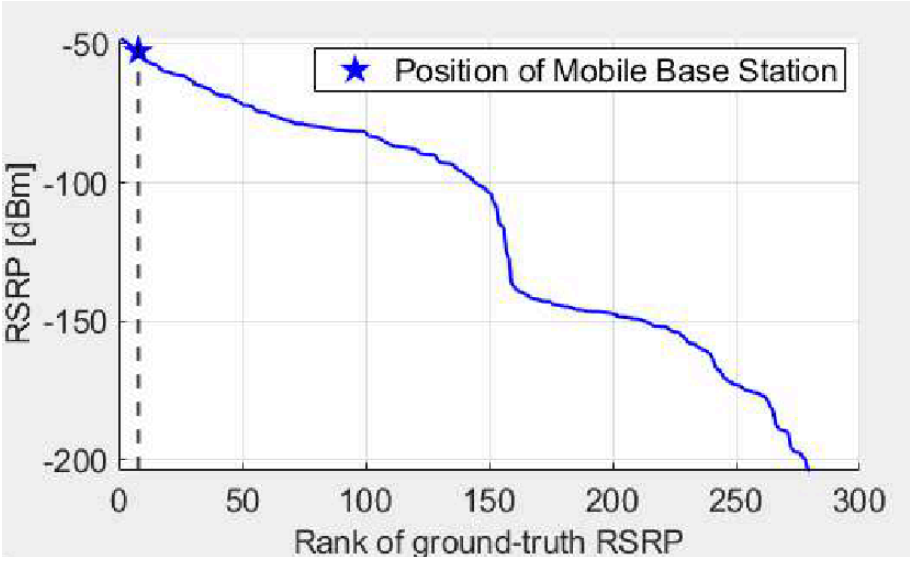

Figure 24: Ground-truth and Predicted RSRP for Two Devices, sorted in descending order of ground-truth RSRP.

Figures 21 and 23 show the corresponding Uncertainty Maps after mobility control. Darker regions indicate areas where uncertainty has been significantly reduced, showing that the sampling process effectively refined the estimated signal distribution.

To further evaluate the accuracy of the estimated RSRP, Figures 24 and 25 compare

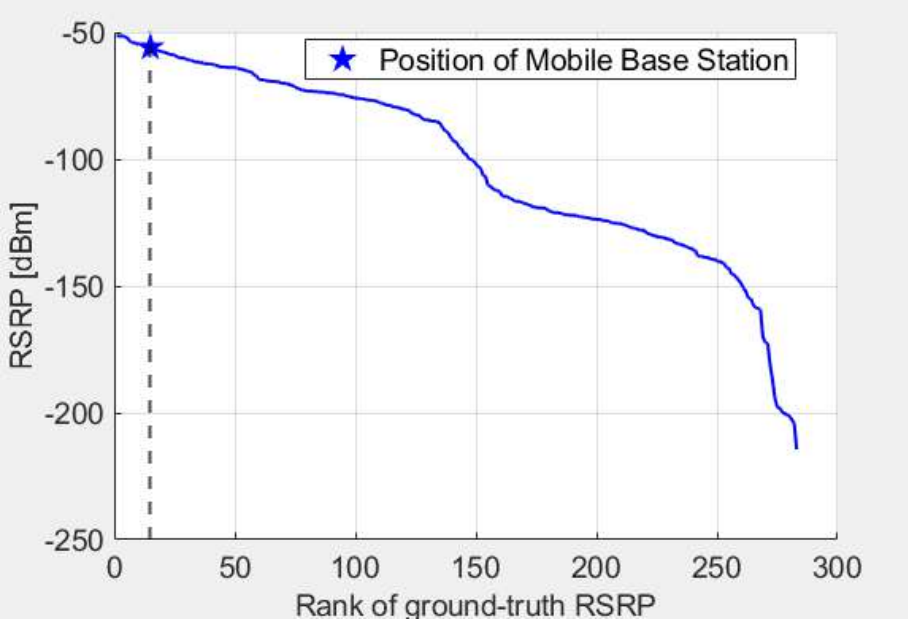

Figure 25: Ground-truth and Predicted RSRP for Three Devices, sorted in descending order of ground-truth RSRP.

the ground-truth and predicted RSRP values after mobility control. The x-axis represents the ranking of ground-truth RSRP values in descending order, while the y-axis shows the RSRP in dBm. By sorting values in this manner, the alignment between the predicted and actual signal distributions becomes clear. The yellow stars mark the locations of the maximum RSRP for both the ground-truth and predicted values, enabling an assessment of how accurately the mobility control method positioned the base station relative to the optimal ground-truth location.

In the two-device case, the estimated maximum RSRP location was within seven grids of the ground-truth maximum RSRP location. Similarly, in the three-device case, the estimated maximum RSRP location was within only four grids of the ground-truth maximum. The efficiency of the method is also evident in its sampling coverage. The two-device case required 70 sampled locations (24.7% of all grids), while the three-device case used 120 sampled locations (42.4%), demonstrating that the method effectively reduces uncertainty with a limited number of samples.

The results confirm that the predicted RSRP closely follows the ground-truth distribution. While minor deviations exist, the base station moves sufficiently close to the optimal

location, demonstrating that the proposed mobility control method effectively optimizes placement and improves communication quality across devices.

5 Conclusion

This thesis proposed and evaluated a dynamic mobility control method for mobile robotic cellular base stations using Bayesian Compressive Sensing (BCS) to construct a Superimposed Signal Map (SSM). The objective was to optimize base station placement dynamically, improving communication quality while maintaining fairness among multiple terminals.

The main contributions of this research are as follows. First, an SSM construction method using BCS was developed, enabling signal strength estimation with limited observation data. Second, a mobility control strategy was introduced, allowing the base station to select movement paths based on the estimated signal distribution. The method effectively balances movement efficiency and communication quality improvements by prioritizing high-uncertainty areas for sampling. Third, simulations in a 5G environment demonstrated that mobility control based on the constructed SSM significantly enhanced communication quality.

The evaluation results confirmed that the proposed method increased the average RSRP by 110.7 dBm in the two-terminal case and 80.9 dBm in the three-terminal case. Additionally, the weakest terminals experienced substantial RSRP gains, reducing communication disparities. The uncertainty reduction process converged after 7 iterations (70 measurement points, covering 24.7% of the total 283 grids) for two terminals and 12 iterations (120 measurement points, covering 42.4%) for three terminals. Visualization of the results further validated that the estimated RSRP closely approximated the ground-truth RSRP distribution. Moreover, the mobile base station successfully moved within seven grids of the ground-truth maximum RSRP location for two terminals and within four grids for three terminals, confirming that the mobility control method guided the base station to a location sufficiently close to the optimal position.

Future work will focus on extending this method to real-world scenarios, particularly in urban and indoor environments where complex radio propagation characteristics, such as multipath fading and obstacles, may impact signal estimation accuracy. Additionally, incorporating environmental sensor data and improving real-time processing will be explored to refine SSM construction further. Another promising direction involves multi-agent mo-

bility control, where multiple mobile base stations collaborate to optimize coverage and network resilience.

By addressing these challenges, the proposed mobility control method has the potential to enhance network adaptability across various applications, including disaster response, large-scale events, and temporary network deployments in next-generation smart cities.

Acknowledgments

I extend my heartfelt appreciation to everyone who supported me in various ways throughout the completion of my master's thesis. I am truly grateful for their invaluable help and encouragement, without which this thesis would not have been possible.

I wish to convey my deepest appreciation to Associate Professor Shin'ichi Arakawa from Osaka University for his invaluable advice, insightful suggestions, and unwavering assistance. His guidance was essential in overcoming the research challenges encountered during this endeavor. Additionally, I am immensely thankful to Professor Masayuki Murata, also from Osaka University, for his invaluable comments and profound insights, which greatly enriched this work. I would also like to express my sincere appreciation to Associate Professor Daichi Kominami, Assistant Professor Tatsuya Otoshi, and Specially Appointed Assistant Professor Masaaki Yamauchi of Osaka University for their numerous valuable contributions. Moreover, I extend my thanks to all the members of the Murata Laboratory for their support.

References

[1] F. Ministry of Agriculture and Fisheries, "Development of smart agriculture," 2022, https://www.maff.go.jp/j/kanbo/smart/#smart.

[2] M. of Internal Affairs and Communications, "Initiatives for utilizing technology in the postal and logistics sector," 2021, https://www.soumu.go.jp/main_content/000762584.pdf.

[3] T. Hirose, F. Nuno, and M. Nakatsugawa, "Development of wireless systems for disaster recovery operations," IEICE Transactions on Electronics, vol. 98, no. 7, pp. 630–635, 2015.

[4] F. Qamar, M. H. S. Siddiqui, K. Dimyati, K. A. B. Noordin, and M. B. Majed, "Channel characterization of 28 and 38 ghz mm-wave frequency band spectrum for the future 5g network," in 2017 IEEE 15th Student Conference on Research and Development (SCOReD), 2017, pp. 291–296.

[5] M. U. A. Siddiqui, F. Qamar, F. Ahmed, Q. N. Nguyen, and R. Hassan, "Interference management in 5g and beyond network: Requirements, challenges and future directions," IEEE Access, vol. 9, pp. 68 932–68 965, Apr. 2021.

[6] S. Ji, Y. Xue, and L. Carin, "Bayesian compressive sensing," IEEE Transactions on Signal Processing, vol. 56, no. 6, pp. 2346–2356, Jun. 2008.

[7] D. Robotics, "Double 3," https://www.doublerobotics.com/double3.html.

[8] "OpenAirInterface," https://openairinterface.org.

[9] "Open5GS open source project of 5GS and EPC," https://open5gs.org.

[10] D. Robotics, "Double 3 developer resources," https://www.doublerobotics.com/developer.html.

[11] S. He and K. G. Shin, "Steering crowdsourced signal map construction via bayesian compressive sensing," in Proceedings of IEEE INFOCOM 2018 - IEEE Conference on Computer Communications, Apr. 2018, pp. 1016–1024.

[12] B. Yang, S. He, and S.-H. G. Chan, "Updating wireless signal map with bayesian compressive sensing," in Proceedings of the 19th ACM International Conference on Modeling, Analysis and Simulation of Wireless and Mobile Systems, Nov. 2016, pp. 310–317.

[13] M. E. Tipping, "Sparse bayesian learning and the relevance vector machine," Journal of Machine Learning Research, vol. 1, no. Jun, pp. 211–244, Jun. 2001.

[14] I. Alawe, A. Ksentini, Y. Hadjadj-Aoul, and P. Bertin, "Improving traffic forecasting for 5G core network scalability: A machine learning approach," IEEE Network, vol. 32, no. 6, pp. 42–49, Nov. 2018.

[15] ETSI, "TS 123 501 V15.2.0 5G: System Architecture for the 5G System (3GPP TS 23.501 Version 15.2.0)," 2018.

[16] A. Aijaz, "Packet duplication in dual connectivity enabled 5G wireless networks: Overview and challenges," IEEE Communications Standards Magazine, vol. 3, no. 3, pp. 20–28, Dec. 2019.